



HAL
open science

PHOTOVOLTAIC-BASED STORAGE-LESS SYSTEM TO SUPPORT ISLANDING IN DISTRIBUTION GRIDS

Candelaria Utrilla, Vincent Debusschere, Hossein D Tafti, Ghias Farivar,
Josep Pou, Nouredine Hadjsaid

► **To cite this version:**

Candelaria Utrilla, Vincent Debusschere, Hossein D Tafti, Ghias Farivar, Josep Pou, et al.. PHOTOVOLTAIC-BASED STORAGE-LESS SYSTEM TO SUPPORT ISLANDING IN DISTRIBUTION GRIDS. CIRED 2021, Sep 2021, Genève, Switzerland. hal-03368972

HAL Id: hal-03368972

<https://hal.science/hal-03368972>

Submitted on 7 Oct 2021

HAL is a multi-disciplinary open access archive for the deposit and dissemination of scientific research documents, whether they are published or not. The documents may come from teaching and research institutions in France or abroad, or from public or private research centers.

L'archive ouverte pluridisciplinaire **HAL**, est destinée au dépôt et à la diffusion de documents scientifiques de niveau recherche, publiés ou non, émanant des établissements d'enseignement et de recherche français ou étrangers, des laboratoires publics ou privés.

PHOTOVOLTAIC-BASED STORAGE-LESS SYSTEM TO SUPPORT ISLANDING IN DISTRIBUTION GRIDS

Candelaria Utrilla^{}, Vincent Debusschere¹, Hossein D. Tafti², Ghias Farivar³, Josep Pou⁴,
Nouredine Hadjsaid¹*

¹*Univ. Grenoble Alpes, CNRS, Grenoble INP, G2Elab, F-38000 Grenoble, France*

²*School of Electrical Engineering and Telecommunications, University of New South Wales, Sydney, Australia*

³*Energy Research Institute @ NTU (ERI@N), Nanyang Technological University, Singapore, Singapore*

⁴*School of Electrical and Electronics Engineering, Nanyang Technological University, Singapore, Singapore*

** maria.utrilla-bustamante@g2elab.grenoble-inp.fr*

Keywords: FLEXIBLE POWER POINT TRACKING, ISLANDING, DISTRIBUTION SYSTEMS, PHOTO-VOLTAIC SYSTEMS

Abstract

Occasionally islanding specific areas of a distribution grid could provide benefits such as the improvement of the grid's reliability and resilience. In the past years, several European distribution system operators have built demonstrators to test islanding on existing distribution grids. These demonstrators have often been based on battery energy storage systems, but the integration of such systems has proven to be burdensome, notably because of their very high costs. This research aims at developing an islanding solution based on already installed photovoltaic (PV) plants and that would require a minimum amount of changes in the existing distribution grids. More specifically, this paper proposes a control structure for a PV-based grid-forming system that can be used as a building block for the pursued islanding solution. A set of simulation results demonstrates that the proposed system is capable of withstanding severe perturbations while functioning in stand-alone mode.

1 Introduction

Even if distribution grids are normally operated in grid-connected mode, it could be advantageous to be able to temporarily disconnect a portion of a distribution grid and operate it in islanded mode (practice that can be designated as "intentional islanding"). The main benefits of this practice are the improvement of both the reliability and the resilience of distribution grids. For instance, if a fault forces to open a feeder, the continuity of supply of the grid placed downstream could be ensured by means of islanding. However, most distribution grids are not technically ready to perform intentional islandings. A common obstacle is the lack of grid-forming units in the area to be islanded. Such units are necessary to fulfil the functions that are normally performed by the main grid: to maintain the generation/consumption equilibrium, while ensuring that the voltage and the frequency are kept within limits.

In the past years, several European distribution system operators have developed demonstrators to test intentional islanding on existing distribution grids [1]. In most of them, battery energy storage systems (BESSs) have been installed in order to perform the necessary grid-forming role. The flexibility of these systems (i.e., they can inject or absorb both active and reactive power) make them specially suitable for this role. In addition, BESSs do not directly emit greenhouse gases unlike some traditional grid-forming units such as diesel generators. Nevertheless, several demonstrators have concluded that BESSs are not easy to integrate in distribution grids, notably because of their very high costs.

On another note, for some years now, the European distribution grids have been experiencing a strong increase of the installed capacity of distributed energy resources. Photovoltaic (PV) plants are, together with wind farms, dominant [2].

In light of these facts, this research aims at developing an islanding solution that would require a minimum amount of changes in current distribution grids (and, therefore, that would minimize the associated costs). The chosen approach is to study if the PV plants already installed in distribution grids can be used to perform the required grid-forming role. Of course, this solution has limitations with respect to a solution using storage. The most relevant one is that the solar resource is non controllable and, therefore, an island can only be created in periods where the solar generation is enough to sustain the power balance of the islanded area. However, it may be a good compromise to improve the reliability and resilience of distribution grids without implementing major changes (the main technical modification would be the update of the firmware of the PV inverters, since most of them can only operate in grid-feeding mode).

More precisely, this paper proposes a control structure for a grid-forming PV system that can be used as a building block for the pursued islanding solution. In addition, the system's response to severe perturbations is tested through dynamic simulations. The paper is structured as follows: Section 2 presents the model of the proposed grid-forming PV system, Section 3 presents the tests results and Section 4 summarizes the conclusions of the study.

2 Model description

Fig. 1 depicts a diagram of the developed PV-based grid-forming system, in which are included both the hardware structure and the control scheme.

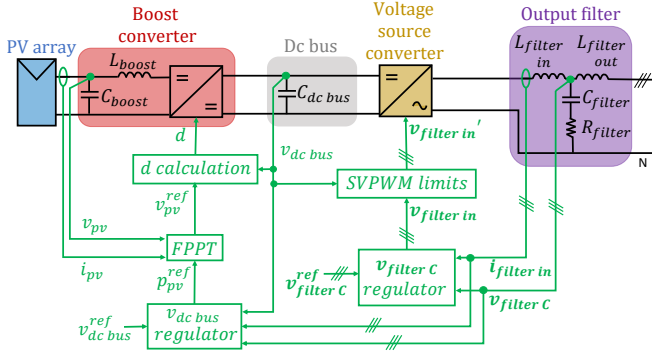


Fig. 1. Schematic of the grid-forming PV system.

2.1 Hardware components

With regard to its physical structure, the system does not differ from a conventional two stage PV inverter [3]. This is the main advantage of the proposed solution: it can be implemented in already installed PV plants, by changing their control firmware.

The PV array has been represented using a single-diode model. The boost converter (BC) and the voltage source converter (VSC) have been built using average models, since the power electronics do not need to be represented in detail. Finally, it must be noted that the ac side of the VSC has four wires (three-phases and neutral), which enable the system to feed single-phase loads. This modeling choice is motivated by the aim of building a system as generic as possible.

2.2 Control strategy

The control scheme of the developed system differs completely from the ones often used in conventional PV plants. In these plants, the PV array is controlled with a maximum power point tracking algorithm (MPPT), which makes the array permanently operate at the maximum point of its power-voltage characteristic (called the maximum power point, MPP). To inject the power generated by the PV array into the grid, the VSC is controlled in grid-feeding mode: i.e., it injects specific amounts of active and reactive power into the grid. And the reference of the active power to inject is imposed by a dc bus regulator, by ensuring that the power coming out of the dc bus (i.e., the active power injected into the grid) is equal to the power coming into the dc bus (i.e., the power produced by the PV array), not considering losses.

In the proposed system, the VSC is controlled in grid-forming mode: it imposes the voltage amplitude and frequency of the islanded grid. For that, a regulator controls the voltage of the filter's middle point ($v_{filter C}$). In particular, the regulator displayed in Fig. 2 has been implemented, since it is a common regulator used for grid-forming systems [4] and it is

specially suited to handle unbalanced loads. The final output of the regulator is the voltage that the VSC should impose at the filter's input ($v_{filter in}$), but Fig. 1 shows that this signal goes through the block *SVPWM limits* before being introduced in the average model of the VSC. This block models the fact that the VSC is not able to generate correct ac voltages if the dc bus voltage ($v_{dc bus}$) is too low. The minimum necessary dc bus voltage depends on: 1) the modulation technique that would be applied to control the power electronics of the VSC, 2) the internal topology of the VSC and 3) the amplitude of the desired ac voltages. In this model, it has been assumed that the VSC is a two-level four-leg device and that a space vector pulse width modulation (SVPWM) technique is used [5].

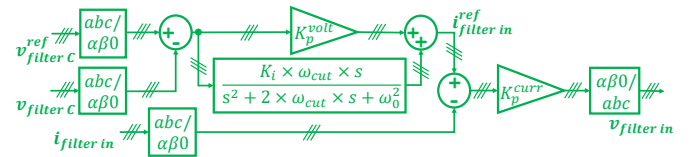


Fig. 2. Implemented VSC voltage regulator.

Furthermore, since the VSC is controlled in grid-forming mode, the active and reactive power injected into the grid can not be fixed by a reference, since they are determined by the loads of the islanded grid. To enable this, the dc bus regulator has been modified: in the proposed system, this regulator determines the PV power reference (p_{pv}^{ref}), ensuring that the power coming into the dc bus (i.e., the power produced by the PV array) is equal to the power going out of it (i.e., the active power demanded by the islanded grid), not considering losses. The structure of the developed dc bus regulator is depicted in Fig. 3. It is observed that the PV power reference is composed by two terms:

- A feedforward term equal to the active power injected by the VSC into the ac side of the system. The term is computed by calculating the instantaneous power going out of the VSC's ac side (p_{ac}) and applying a moving average, which eliminates the oscillations that appear in the instantaneous power when the loads are unbalanced.
- A feedback term, that ensures that the dc bus voltage is regulated to its reference value. It must be pointed out that, in case of an unbalanced load, the oscillations in the instantaneous ac power would cause oscillations in the dc bus voltage too. In consequence, a moving average is also applied to the signal $v_{dc bus}$, so that the oscillations do not transfer to the PV power reference.

Finally, the saturation block of the dc bus regulator impedes the PV power reference to get a value higher than the rated power of the system or lower than zero. Actually, if the PV power was negative, the array would consume power. But this would not be allowed by a real BC (the internal diode would prevent the power transfer from the dc bus to the PV array).

The last major change with respect to conventional PV systems concerns the control of the PV array. In the proposed system, the power produced by the PV array has to be adapted

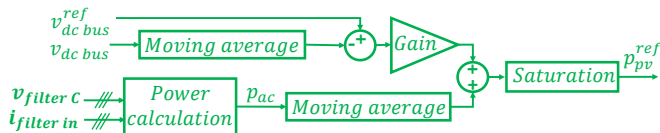


Fig. 3. Proposed dc bus voltage regulator.

to the active power consumed by the islanded grid. To achieve this, the MPPT has been substituted by a flexible power point tracking algorithm (FPPT), which allows to use the PV array at different operating points (and not only at the MPP). The FPPT algorithm proposed in [6] has been implemented. This algorithm is executed with a constant periodicity, taking as inputs the PV power reference calculated by the dc bus regulator and measurements of the PV array's voltage (v_{pv}) and current (i_{pv}). Each time it is executed, the FPPT:

1. Decides if a small or a large voltage step should be applied to the terminals of the PV array. This depends on the difference between the PV power reference and the PV actual power ($p_{pv} = v_{pv} \times i_{pv}$). In essence, if the difference is big, it considers that the system is in transient state and chooses a large voltage step. If the difference is small, it considers that the system is in steady state and chooses a small step.
2. Determines the PV voltage reference (v_{pv}^{ref}), by either adding or subtracting the calculated voltage step to the measured PV voltage. This choice depends on the selected operating region of the PV array. For example, if the PV array power has to be increased and system is operating at the right side of the MPP (characterized by a negative power-voltage slope), the PV voltage should be decreased.

Finally, the PV voltage reference is used by the d calculation block to calculate the duty cycle (d) to be applied to the BC ($d = 1 - v_{pv}^{ref} / v_{bus\ dc}$).

3 Simulation results

This section presents the results obtained with two simulations in which the proposed grid-forming PV system is subjected to severe perturbations. The simulations have been performed in MATLAB/Simulink™. In both of them, the system feeds the islanded grid depicted on Fig. 4, which consists on:

- A first load represented by a set of switching resistors, that allow to easily execute steps of the active power consumed by the islanded grid.
- A second load represented by an induction motor, which is a dynamic load very common in distribution grids.
- Finally, a distribution line, represented with an RL model.

Fig. 4 also displays some variables of the islanded grid: the voltage at the loads terminals (v_{loads}), the current absorbed by the switching resistors ($i_{resistors}$), the current absorbed by the motor (i_{motor}) and the motor's rotation speed (ω_{motor}).

Table 1 and Table 2 summarize, respectively, how the parameters of the grid-forming PV system and of the islanded grid have been configured for the simulations. It is important to

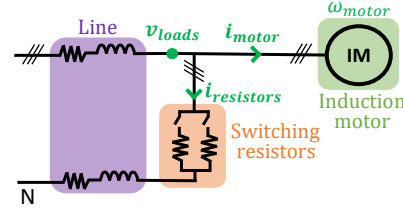


Fig. 4. Implemented islanded grid model.

underline that the physical components of the grid-forming PV system have been sized as in conventional PV inverters, so that the model fairly represents the hardware components of an existing PV plant. Finally, Fig. 5 depicts the power-voltage characteristics of the simulated PV array.

3.1 Test 1: Large load step

In this test, the irradiance and temperature are maintained, respectively, at 1000 W/m^2 and 25°C . Under these conditions, the available PV power (i.e., the power at the MPP) is of 14.72 kW . Initially, the active power consumed by the islanded grid represents just 12% of this power (5% is consumed by a three-phase resistor, 6% by the motor and 1% is dissipated in the line). At $t = 0.25 \text{ s}$, a new three-phase resistor is connected, giving rise to a drastic increase of the active power consumed by the islanded grid (it becomes 93% of the available PV power). It must be noted that the three phases of the ac side are kept balanced at all times. Fig. 6 displays various resulting curves of the dc side of the system.

Table 1 Parameters of the grid-forming PV system.

Ratings			
Grid voltage	400 V	Dc bus voltage	800 V
Grid frequency	50 Hz	Power	15 kVA
Physical components			
L_{boost}	9.8 mH	$L_{filter\ out}, L_{filter\ in}$	3 mH
C_{boost}	13.1 μF	C_{filter}	3.2 μF
$C_{dc\ bus}$	4 mF	R_{filter}	7.2 Ω
FPPT			
Time step	0.015 s	$V_{step\ transient}$	26 V
$\Delta p_{threshold}$	2250 W	$V_{step\ steady-state}$	5 V
$ \Delta p / \Delta v _{threshold}$	27 W/V	Operating region	Right
$v_{dc\ bus}$ regulator			
Mov. aver. period	0.02 s	Gain	50 W/V
$v_{dc\ bus}^{ref}$	800 V		
$v_{filter\ C}$ regulator			
K_p^{volt}	0.035	ω_0	314 rad/s
K_i	25	K_p^{curr}	100
ω_{cut}	10 rad/s	$v_{filter\ C}^{ref}$	1.05 p.u.

Table 2 Parameters of the islanded grid.

Induction motor			
Nom. voltage	400 V	Nom. power	7.5 kW
Nom. frequency	50 Hz	Poles pairs	2
Inertia constant	0.2 s	Friction factor	0 p.u.
Stator resistance	0.035 p.u.	Rotor resistance	0.035 p.u.
Stator inductance	0.045 p.u.	Rotor inductance	0.045 p.u.
Mutual inductance	1.827 p.u.		
Line			
Resistance	2.2 Ω/km	Length	0.5 km
Reactance	0.08 Ω/km		

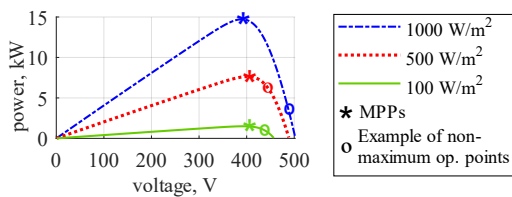


Fig. 5 Power-voltage characteristics of the simulated PV array (the temperature is 25° C for all curves).

Before the load step, p_{ac} is kept constant and, by means of the dc bus controller and the FPPT, p_{pv} oscillates around p_{ac} . Thanks to this, $v_{dc\ bus}$ is kept around its reference value. Right after the load step, the feedforward branch of the dc bus controller quickly increases p_{pv}^{ref} , so that it matches the new value of p_{ac} . In consequence, the FPPT starts increasing p_{pv} soon after the load step. However, the initial difference between p_{ac} and p_{pv} makes $v_{dc\ bus}$ considerably decrease. Therefore, the feedback branch of the dc bus controller comes into play, increasing p_{pv}^{ref} over p_{ac} in order to bring $v_{dc\ bus}$ back to its reference value. Still, it can be observed that p_{pv} is not able to

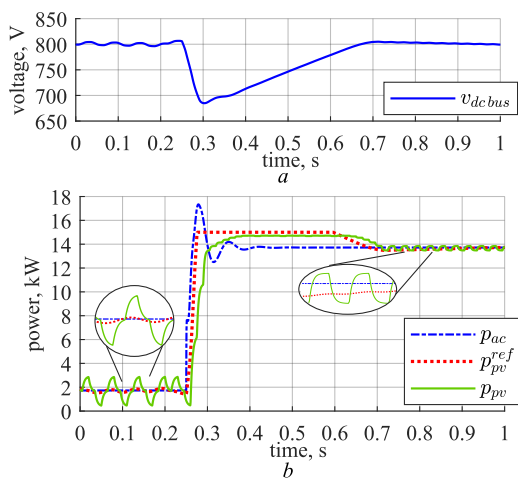


Fig. 6 Test 1: (a) dc bus voltage; (b) instantaneous power consumed by the islanded grid, PV reference power and PV actual power.

follow p_{pv}^{ref} between $t = 0.4$ s and $t = 0.6$ s, because the PV array reaches its MPP. During this period, the FPPT maintains the PV array at the MPP and, since p_{pv} is slightly bigger than p_{ac} , $v_{dc\ bus}$ increases slowly towards its reference value.

Regarding the ac side, since the undervoltage of $v_{dc\ bus}$ is not very pronounced, the VSC is capable of generating correct ac voltages at all times (to impose a balanced voltage of 1.1×400 V at $v_{filter\ in}$, the necessary dc bus voltage is $1.1 \times 400 \times \sqrt{2} \approx 622$ V). The motor experiences small speed oscillations at the instant when the load steps take place (the overshoot is smaller than 2%), but these are damped and the motor keeps working in a stable operating point afterwards.

It can be concluded that the system withstands abrupt load variations: an ac power step of +81 % leads to a temporary undervoltage of 685 V at the dc bus (which does not impede the VSC or the BC to function properly).

3.2 Test 2: Abrupt irradiance dip

In this test, the irradiance and the temperature have initial values of 1000 W/m² and 25° C (available PV power of 14.72 kW). The loads are balanced and the islanded grid consumes 98 % of the available power: 34 % is consumed by a three-phase resistor, 54 % is consumed by the motor and 10 % is dissipated in the line. From $t = 0.5$ s, the irradiance experiences the 2 s dip depicted on Fig. 7 (which can represent, for example, the passage of a cloud). It is important to point out that the irradiance ramps that configure the dip are very pronounced [7]. Fig. 8 and Fig. 9 display various resulting curves of the dc side and of the ac side of the system.

At $t = 0.5$ s, the irradiance negative ramp causes the linear decrease of p_{pv} , which causes the drop of $v_{dc\ bus}$. At $t \approx 1.6$ s, $v_{dc\ bus}$ goes under the limit value at which the VSC is not capable of creating the desired voltages on its ac side. In consequence, both $v_{filter\ in}$ and v_{loads} start decreasing too. However, the irradiance positive ramp that starts at $t = 1.5$ s makes p_{pv} increase and, from $t \approx 1.8$ s, it becomes again bigger than p_{ac} , which makes $v_{dc\ bus}$, $v_{filter\ in}$ and v_{loads} recover their correct values.

It can be considered that the system withstands the irradiance dip. The dc bus undervoltage (571 V) does not perturb the BC. And, although the islanded grid is affected by this undervoltage, the minimum voltage at the loads terminals is tolerable (0.85 p.u.) and it does not make the induction motor unstable. It must be underlined that, if the proposed system was less stressed, it would be able to withstand longer irradiance dips. For instance: with a smaller motor (3 kW of nominal power), softer irradiance ramps (± 50 W/m²) and a more advantageous initial condition (islanded grid consuming 50% of the available power), the system can withstand 23 s voltage dips.

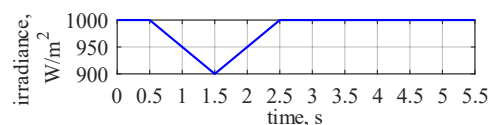


Fig. 7. Test 2: irradiance variation.

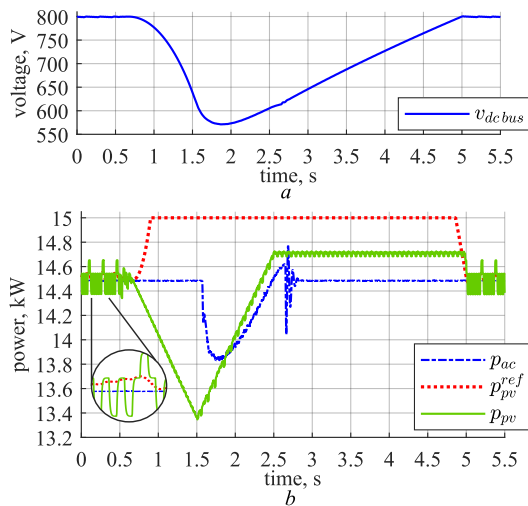


Fig. 8 Test 2: (a) dc bus voltage; (b) instantaneous power consumed by the islanded grid, PV reference power and PV actual power.

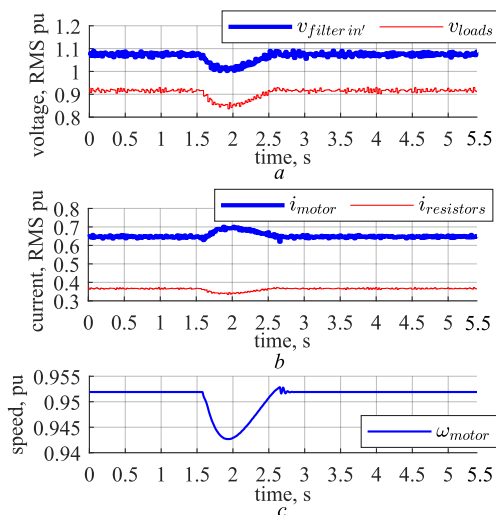


Fig. 9 Test 2: (a) voltage imposed by the VSC and voltage at the loads' terminals; (b) current absorbed by the motor and by the switching resistors; (c) speed of the motor.

4 Conclusion

This paper has presented a control structure for a PV-based grid-forming system. It has been proven that, if there is enough solar resource, the proposed system can withstand severe load perturbations. Moreover, it has been shown that the system has a certain capability of withstanding irradiance dips. These facts corroborate that the proposed system could be a good solution to create islands in distribution grids without undertaking major investments. The downside of this solution is that the islands can only be created when the solar resource is enough to guarantee the power balance of the island. Nonetheless, in distribution grids with high PV penetration, the islanding duration

provided by this solution could be enough to perform a quick maintenance or to transport diesel generators to the area. If a more complete islanding scheme was required, the proposed solution could be complemented with a BESS, but the flexibility provided by the grid-forming PV units would allow to minimize the BESS's size. This is a potential subject for further investigations.

5 Acknowledgements

This work has been funded in the scope of the NTU – CNRS “Excellence Science” Joint Research Program.

6 References

- [1] 'i-DE launches the first battery storage system for electricity grids in Spain', <https://www.iberdrola.com/press-room/news/detail/i-de-launches-first-battery-storage-system-electricity-grids-spain>, accessed 23 February 2021
- [2] Prettico, G., Flammini, M.G., Andreadou, N., et al.: 'Distribution System Operators observatory 2018 - Overview of the electricity distribution system in Europe' (Publications Office of the European Union, 2019)
- [3] Xiao, W.: 'Photovoltaic Power System: Modeling, Design, and Control' (Wiley, 2017)
- [4] Liu, Q., Caldognetto, T., Buso, S.: 'Review and Comparison of Grid-Tied Inverter Controllers in Microgrids', *IEEE Transactions on Power Electronics*, 2020, 35, (7), pp. 7624-7639, doi:10.1109/TPEL.2019.2957975
- [5] Shen, D., Lehn, P.W.: 'Fixed-frequency space-vector modulation control for three-phase four-leg active power filters', *IEE Proceedings - Electric Power Applications*, 2002, 149, (4), pp. 268-274, doi:10.1049/ip-epa:20020377
- [6] Tafti, H.D., Sangwongwanich, A., Yang, Y., et al.: 'A general algorithm for flexible active power control of photovoltaic systems'. 2018 IEEE Applied Power Electronics Conference and Exposition (APEC), San Antonio, TX, USA, 2018, pp. 1115-1121, doi:10.1109/APEC.2018.8341156
- [7] Bründlinger, R., Henze, N., Häberlin, H., et al.: 'prEN 50530 – The new European standard for performance characterisation of PV inverters'. 24th European Photovoltaic Solar Energy Conference, Hamburg, Germany, 21-25 September 2009, pp. 3105-3109, doi:10.4229/24thEUPVSEC2009-4EP.1.2